Inactivation of Pyruvate Formate-Lyase by Dioxygen: Defining the Mechanistic Interplay of Glycine 734 and Cysteine 419 by Rapid Freeze-Quench EPR†

Wenhai Zhang,‡ Kenny K. Wong,‡ Richard S. Magliozzo,§ and John W. Kozarich*,‡

Department of Chemical Biology, Merck Research Laboratories, Rahway, New Jersey 07065-0900, and Department of Chemistry, Brooklyn College of CUNY, Brooklyn, New York 11210

Received November 9, 2000; Revised Manuscript Received January 30, 2001

ABSTRACT: Pyruvate formate-lyase from *Escherichia coli* (EC 2.3.1.54; PFL) catalyzes the reversible anaerobic conversion of pyruvate and CoA into acetyl-CoA and formate. Active PFL contains a novel α-carbon centered glycyl radical at G734 that is required for its catalytic activity. Two adjacent cysteine residues, C418 and C419, are essential for PFL activity according to site-directed mutagenesis studies. Upon exposure to air, active PFL loses its activity with the concomitant loss of the glycyl radical. Previous EPR studies of dioxygen inactivation of PFL revealed protein-based peroxyl and sulfinyl radicals during the manual mixing and quenching process [Reddy et al. (1998) *Biochemistry 37*, 558−563]. To probe the mechanism of this process, we carried out experiments using rapid freeze-quench EPR spectroscopy. Upon mixing of active wild type or C418A PFL with oxygenated solution, a short-lived radical intermediate appears at the earliest time point (10 ms), followed by the appearance of a long-lived sulfinyl radical. The axial EPR spectrum of this short-lived radical ($g = 2.034, 2.007$) is characteristic of a peroxyl radical. When C419A PFL or the double mutant [C418A/C419A] PFL was mixed with oxygenated solution, the peroxyl radical was also observed at 10 ms but in this case persisted over 12 s. These observations provide compelling evidence to support a proposed mechanism in which dioxygen quenches the glycyl radical in the active enzyme and the resulting peroxyl radical may react further with the sulfhydryl group of the C419 residue to form the sulfinyl radical.

Pyruvate formate-lyase from *Escherichia coli* (EC 2.3.1.54; PFL)[1] is the prototype of the family of glycyl radical enzymes that contains enzymes such as the class III ribonucleotide reductase (*1*) and benzylsuccinate synthase (*2*). PFL is found in a variety of facultative anaerobes where it catalyzes the reversible anaerobic conversion of pyruvate and coenzyme A (CoA) to acetyl-CoA and formate (*3*).

This reaction follows ping-pong kinetics with acetylated PFL as an isolable intermediate (*3*). The active site of the enzyme contains an α-carbon centered radical, located at glycine 734, which is required for its catalytic activity (*4*−*6*). Two cysteine residues, C418 and C419, are also found to be essential for catalysis by site-directed mutagenesis but are not required for generation and subsequent stabilization of the glycyl radical (*7*, *8*). X-ray crystal structures of PFL corroborate functional roles for C419 and C418 on the basis of their spatial proximity to G734 (*9*, *10*).

PFL is a homodimer of 85-kDa monomers and is inactive if purified under aerobic conditions (*11*, *12*). The conversion of inactive PFL to its active form is achieved by another enzyme, PFL-activating enzyme (AE), under strictly anaerobic conditions. AE requires *S*-adenosyl-L-methionine (AdoMet) and flavodoxin, or photoreduced 5-deazariboflavin as cosubstrates. Pyruvate or oxamate is also required as an allosteric effector for PFL (*13*, *14*).

The active enzyme is rapidly inactivated by oxygen (*6*), and this reaction has played an important role in understanding the PFL catalytic mechanism. Oxygen inactivation was used to define the glycyl radical site in the active enzyme since it results in the cleavage of the protein into fragments of 82 and 3 kDa (*6*). Amino acid sequencing of the fragments established G734 as the site of the radical. A recent EPR investigation of the mechanism of the inactivation in wild type and mutant PFL enzymes revealed the formation of two protein-based radical intermediates for samples exposed to O_2 for ∼30 s (*15*). A sulfinyl radical (RSO•) was observed in wild type PFL and C418A mutant, suggesting that it is derived from C419 (see Figure 1). In contrast, only a peroxyl radical (ROO•) was found in C419A and C418A/C419A PFL mutants, suggesting that this radical is located at G734. Combined with evidence that C419 is involved in solvent hydrogen exchange into the glycyl radical (*8*), these data suggested that G734 and C419 have a close spatial relationship and their interaction is mechanistically important. This proximity has been confirmed by recent crystallographic studies (*9*, *10*).

A mechanism that accounts for the formation of the radical intermediates was thus proposed (Scheme 1) (*15*), and its

† This research was supported in part by NIH Grant AI43582 to R.S.M.

* To whom correspondence should be addressed. Phone: 732-594-3249, Fax: 732-594-3695. E-mail: john_kozarich@merck.com.

‡ Merck Research Laboratories.

§ Brooklyn College of CUNY.

[1] Abbreviations: PFL, pyruvate formate-lyase; AE, PFL activating enzyme; DTT, dithiothreitol; CoA, coenzyme A; acetyl-CoA, acetyl-coenzyme A; AdoMet, *S*-adenosyl-L-methionine; Tris, tris(hydroxymethyl)aminomethane; IPTG, isopropyl-β-D-thiogalactopyranoside; Hepes, *N*-(2-hydroxyethyl)piperazine-*N*′-2-ethanesulfonic acid; EPR, electron paramagnetic resonance; RFQ, rapid freeze-quench.

10.1021/bi002589k CCC: $20.00
Published on Web 03/08/2001

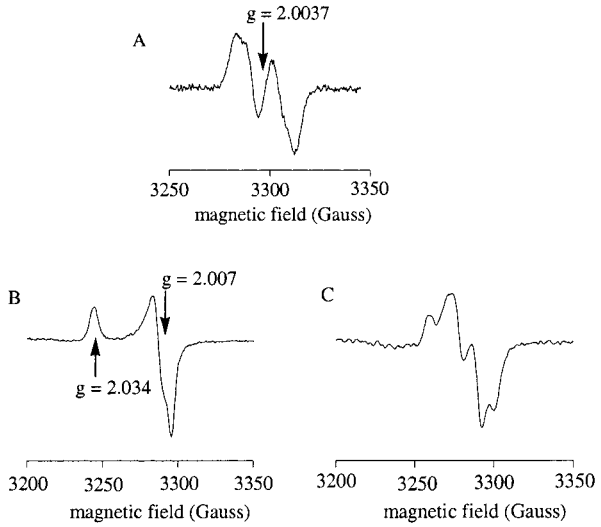

FIGURE 1: (A) EPR spectrum of the glycyl radical of wild-type PFL; (B) EPR spectrum of peroxyl radical formed from exposure of active C418A/C419A PFL to air; (C) EPR spectrum of sulfinyl radical formed by exposure of active wild-type PFL to air. Spectra were taken at microwave frequency 9.230 GHz [Adapted from Reddy et al. (*15*)].

Scheme 1: Proposed Mechanism of PFL Inactivation by Dioxygen (Adapted from Reddy et al., ref *15*)

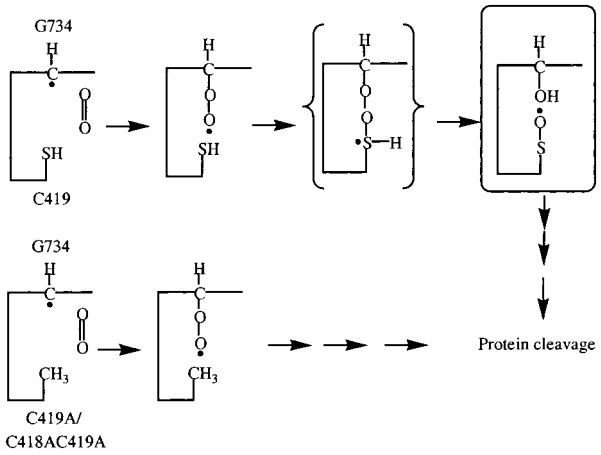

Scheme 2: Alternate Reaction Pathway in the Dioxygen Inactivation of Pyruvate Formate-Lyase (Adapted from Gauld and Eriksson, ref *16*)

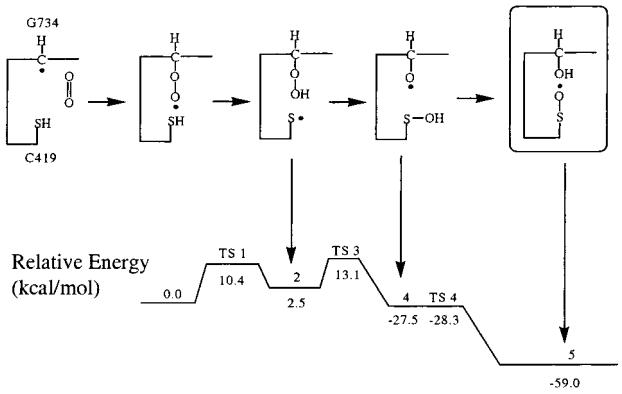

feasibility was investigated in recent theoretical calculations (Scheme 2) (*16*). To probe further the process of oxygen inactivation, we now report our studies of wild type and mutant PFLs using freeze-quench EPR spectroscopy. Our findings further define the mechanistic sequence of oxygen inactivation of PFL and highlight the utility of rapid freeze-quench EPR for understanding the radical chemistry of this emerging class of glycyl radical enzymes.

MATERIALS AND METHODS

All chemicals were obtained from Aldrich or Sigma and were used without further purification. 5-Deazariboflavin was a gift of Merck Research Laboratories.

Enzyme Preparations. Recombinant PFL was purified from *E. coli* BL21 (*17*) (Novagen) bearing pKKBWM5.5C, a construct of pKK223-3 (Pharmacia) and *pfl* under the control of the *tac* promotor. IPTG (0.2 mM) was added to cell cultures at mid-log phase for protein induction. The purification of PFL was based on the procedure of Reddy et al. (*15*). C418A, C419A, and C418A/C419A mutant enzymes were purified using techniques similar to those used for wild type PFL. C418S and C419S mutant enzymes were similarly purified from *E. coli* strain N4830 (*8*). Protein concentrations were determined by the method of Bradford (*18*) using a kit purchased from Bio-Rad. Recombinant AE was purified from *E. coli* strain N4830 (*14*). AE in the soluble fraction was partially purified by phenyl-sepharose chromatography.

Activation of PFL. Recombinant PFL, C418A, C419A, C418AC419A, and C419S mutant enzymes were activated by a modified published procedure (*15*). Typically, the activation mixture contained 100 mM Hepes/100 mM KCl, pH 7.5, 1.5 mM AdoMet, 50 μM 5-deazariboflavin, 6 mM DTT, 20 mM oxamate, 0.4 mM Fe (II), 50 μg/mL AE, and 10 mg/mL PFL or the mutant enzyme in a final volume of 3 mL. After all the components were mixed, the solution was transferred to a 3.5-mL vari-clean vial (Pierce) and was degassed with oxygen-free argon at room temperature. Activation was initiated by photoreduction of 5-deazariboflavin using illumination from a 100 W xenon lamp situated 30 cm from the sample. Gentle stirring was applied to the activation mixture to ensure even illumination. The activation time was typically 1 h, after which the samples were placed on ice and transferred to a Type C anaerobic chamber (Coy Laboratory). Activation of PFL was confirmed by transferring 200 μL of activation mixture to an argon purged septum-sealed EPR tube (Wilmad) using a gastight syringe and quickly freezing the solution in liquid nitrogen for EPR measurement at 77 K. The activated PFL was then transferred in the glovebox to the 2-mL gastight drive syringe of the freeze-quench instrument (Update Instrument, Inc.). Several control samples containing all the activation components, except AdoMet, AE, or 5-deazariboflavin, were activated under similar experimental conditions as described previously (*15*).

Activation of Acetylated PFL. The active acetylated PFL was obtained by activating PFL as above except using 20 mM pyruvate instead of oxamate as the allosteric effector.

Preparation of Oxygenated Buffer. Oxygenated buffer used in the rapid freeze-quench experiments was made by purging 100 mM Hepes/100 mM KCl buffer at pH 7.5, with pure oxygen gas at room temperature (*19*). The concentration of oxygen in this solution was estimated to be ~1.0 mM at room temperature (*20*). The oxygenated buffer then was transferred to the 2-mL gastight drive syringe of the freeze-quench instrument in the open air.

Preparation of RFQ-EPR Samples. Rapid freeze-quenching experiments were carried out using an Update Instrument System 1000 with quenching bath provided by the same vendor. PFL solutions were mixed with oxygenated buffer in a 1:1 (v/v) ratio. Mixing was performed at room temperature, and reactions were quenched at various times after mixing (10 ms to 15.2 s) by freezing in isopentane at −140 °C. Quenched samples were then packed into quartz EPR tubes and stored in liquid nitrogen. EPR analysis was usually performed on the same day.

Electron Paramagnetic Resonance Spectroscopy. EPR spectra were recorded at X-band using a Varian E-12 spectrometer interfaced to a personal computer. Samples were placed in a liquid nitrogen coldfinger Dewar for EPR measurement at 77 K. Data acquisition and manipulation was achieved using WinEPR software as described in ref *21*. Experimental conditions were as follows: microwave frequency 9.150 GHz; field modulation frequency: 100 kHz; modulation amplitude, 3.2 G; microwave power, 0.05 or 2 mW.

Estimation of the percentage of total intensity of each intermediate species observed using the freeze-quench technique was achieved (using SigmaPlot software) by "synthesizing" by summation the observed multicomponent EPR spectrum for each sample frozen at the indicated time points during the oxygen inactivation experiments. The constituent spectra used for this synthesis were digitized data sets acquired from samples exhibiting the spectrum of only one of the three species of interest (glycyl radical, peroxyl radical, sulfinyl radical), each of which was normalized to a constant intensity. In this manner, fractional contributions of each normalized spectrum could be summed and the resulting function plotted for comparison to the data. Superposition of the synthesized spectrum with the data allowed for very good evaluation of the relative contribution of the component spectra in those cases where only two species were involved and the error was estimated to be less than or equal to 5%. For the early time points in the experiment using wild-type PFL (and acetyl-PFL, and C418A PFL), three components were involved, making the procedure less accurate. Error estimates here are less than or equal to 10%. Plots of the relative contribution of each component species to the total observed EPR spectra were then made.

RESULTS

Oxygen Inactivation of Wild-Type PFL. The EPR spectrum of active PFL is a doublet at $g = 2.0037$ arising from a glycyl radical located at residue G734 with the principal splitting due to the α-hydrogen atom (Figure 1, panel A) (*15*). This radical was not observable in any of the control samples described in the Experimental Section, consistent with an earlier report (*15*). The active enzyme is rapidly inactivated when exposed to oxygen, resulting in loss of the glycyl radical and protein fragmentation. Previous EPR results by manual mixing of active wild type and mutant enzymes with oxygenated solutions suggested a reaction pathway in which a protein-based peroxyl radical preceded a protein-based sulfinyl radical detected about 30 s after mixing (*15*). Here, RFQ-EPR spectroscopy was used to test the proposed mechanism. Rapid freeze-quenching of activated wild-type

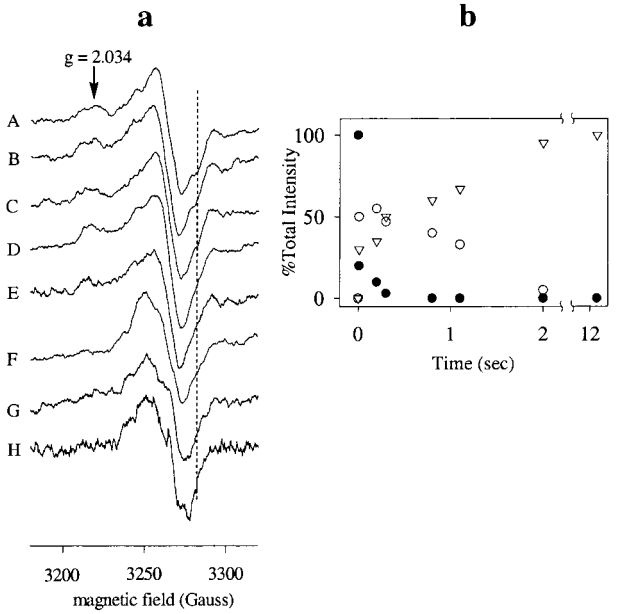

FIGURE 2: (a) Time-course of the oxygen inactivation of activated wild-type PFL with oxygenated buffer. 56 μM active wild-type PFL in anaerobic buffer (100 mM Hepes, 100 mM KCl, 6 mM DTT, pH = 7.5) was mixed at room temperature with 1 mM oxygenated buffer (100 mM Hepes, 100 mM KCl, pH = 7.5). The reaction was quenched at (A) 0.01 s, (B) 0.2 s, (C) 0.3 s, (D) 0.8 s, (E) 1.1 s, (F) 2.0 s, (G) 5.0 s, and (H) 12.2 s. The vertical dashed line indicates residual glycyl radical. (b) The time-course of % total intensity of each species (●, glycyl radical; ○, peroxyl radical; ▽, sulfinyl radical).

PFL mixed with oxygenated solution demonstrated that some glycyl radical persisted through 300 ms, evidenced by the glycyl radical feature on the high field edge of the spectrum (see dashed line) (Figure 2, panel a, spectra A−C). However, as early as 10 ms, a new radical signal appeared (Figure 2, panel a, spectrum A). The feature at $g = 2.034$ is a characteristic component of the axial signal due to a proposed carbon centered peroxyl radical (Figure 1, panel B) (*15*). This feature is observable through 2 s reaction time (Figure 2, panel a; see Figure 2, panel b, for quantitation of species). In the spectrum of a sample freeze-quenched at 12.2 s after mixing (Figure 2, panel a, spectrum H), the disappearance of the peroxyl radical component is complete and the observed spectrum is consistent with the formation of a sulfinyl radical.

Oxygen Inactivation of C418A PFL. Previous studies of solvent hydrogen exchange and oxygen inactivation by manual freeze-quenching demonstrated that residue C419 mediates the solvent exchange and is also the location of the sulfinyl radical (*10*, *15*). When C418A PFL was activated and mixed with oxygenated buffer, the glycyl radical persisted from 10 ms to 0.3 s but disappeared after prolonged reaction periods (Figure 3, panel a). The low field feature of the peroxyl radical is observable at 10 ms and becomes quite prominent at 0.8 s (Figure 3, panel a, spectra A−D). The peroxyl radical feature persists through 2 s and the sulfinyl radical spectrum becomes apparent at 15.2 s (Figure 3, panel a, spectra E−G; Figure 3, panel b). The apparently similar lifetime of the peroxyl radical in C418A and wild type PFL suggests that the mutation of cysteine 418 to alanine does not significantly affect transfer of the radical species from the initially formed peroxyl radical to the sulfur-

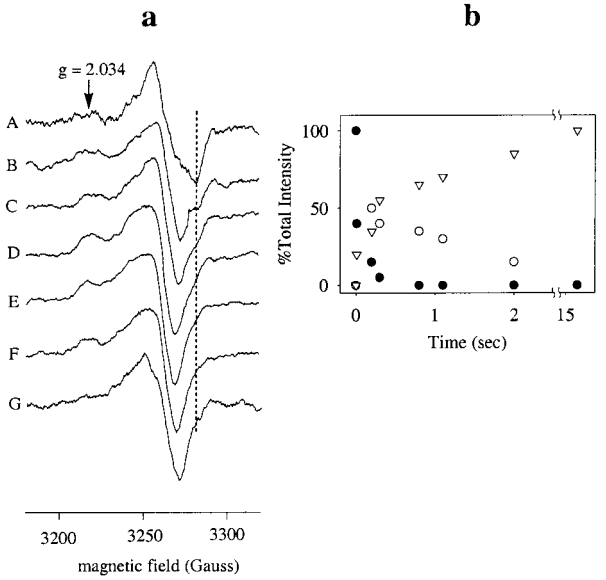

FIGURE 3: (a) Time-course of the oxygen inactivation of activated C418A PFL with oxygenated buffer. 56 μM active C418A PFL in anaerobic buffer (100 mM Hepes, 100 mM KCl, 6 mM DTT, pH = 7.5) was mixed at room temperature with 1 mM oxygenated buffer (100 mM Hepes, 100 mM KCl, pH = 7.5). The reaction was quenched at (A) 0.01 s, (B) 0.2 s, (C) 0.3 s, (D) 0.8 s, (E) 1.1 s, (F) 2.0 s, and (G) 15.2 s. The vertical dashed line indicates residual glycyl radical. (b) The time-course of % total intensity of each species (●, glycyl radical; ○, peroxyl radical; ▽, sulfinyl radical).

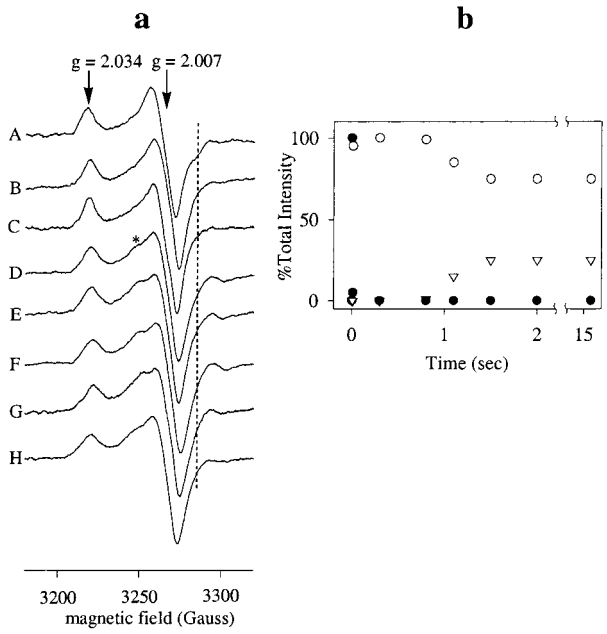

FIGURE 4: (a) Time-course of the oxygen inactivation of activated C419A PFL with oxygenated buffer. 56 μM active C419A PFL in anaerobic buffer (100 mM Hepes, 100 mM KCl, 6 mM DTT, pH = 7.5) was mixed at room temperature with 1 mM oxygenated buffer (100 mM Hepes, 100 mM KCl, pH = 7.5). The reaction was quenched at (A) 0.01 s, (B) 0.3 s, (C) 0.8 s, (D) 1.1 s, (E) 1.5 s, (F) 2.0 s, (G) 5.0 s, and (H) 15.2 s. The vertical dashed line indicates residual glycyl radical. The feature marked with (*) is tentatively assigned as a C418-based sulfinyl radical. (b) The time-course of % total intensity of each species (●, glycyl radical; ○, peroxyl radical; ▽, sulfinyl radical).

based radical as proposed for wild-type enzyme (Scheme 1).

Oxygen Inactivation of C419A PFL. When active C419A PFL and oxygenated buffer were mixed and freeze-quenched, a spectrum characteristic of peroxyl radical was also observed as early as 10 ms (Figure 4, panel a, spectrum A). The spectrum of this radical is similar to that of the peroxyl radical observed in our earlier study with manually quenched C419A (*15*). Only a small remnant of glycyl radical signal was observed at 10 ms, evidenced by a shoulder indicated by a dashed line, demonstrating nearly complete conversion of the glycyl radical to a peroxyl radical at the earliest time point achievable by our methodology. The feature representing the glycyl radical disappeared by 0.3 s (Figure 4, panel a, spectrum B). The peroxyl radical signal persists through 15 s (Figure 4, panel a, spectra C-H), consistent with earlier observations (*15*). Interestingly, a shoulder marked with (*) was clearly observable at 1.1 s and remained relatively stable through 15 s. We are not certain of the identity of this feature; however, it is not observed in the C418AC419A PFL (vide infra), suggesting that it may represent a slow and partial formation of sulfinyl radical at C418 (see Figure 4, panel b, for quantitation).

Oxygen Inactivation of C419S PFL. The oxygen inactivation of another C419 mutant was also investigated. Active C419S PFL was freeze-quenched with oxygenated buffer as described above. This reaction also resulted in the formation of a peroxyl radical at 10 ms and the complete disappearance of glycyl radical by 0.3 s (Figure 5, panel a, spectra A−C). A similar shoulder marked with (*) near $g = 2.007$ that was observed in C419A PFL oxygen inactivation was also observable in the C419S PFL reaction profile from 0.55 to 5 s (Figure 5, panel a, spectra D−I), suggesting a common side-reaction pathway that may involve C418 in these two C419 mutants (see Figure 5, panel b, for quantitation).

Oxygen Inactivation of C418AC419A PFL. As above, freeze-quenching at 10 ms revealed the low field feature of a peroxyl radical at $g = 2.034$ together with the starting glycyl radical spectrum (Figure 6, panel a, spectrum A). The $g = 2.034$ feature of the peroxyl radical becomes prominent at 0.2 s and the glycyl radical feature is no longer observable by 1.5 s reaction time (Figure 6, panel a, spectra B−F). The spectrum of the peroxyl radical remains essentially unchanged through 15 s. In duplicate experiments, the disappearance of the glycyl radical was somewhat slower than that in the other enzymes studied (~3-fold slower; Figure 6, panel b). It is unclear if this represents a slight procedural difference in the experiment or if it is due to a small structural reorganization of the active site in the double mutant that results in a change in accessibility of the glycyl radical to oxygen.

Oxygen Inactivation of Acetylated PFL. Acetylated enzyme is an isolable intermediate in the PFL reaction (*3*). The effect of acetylation on the oxygen inactivation process was tested and the reaction profile is shown in Figure 7 (spectra A−G). The $g = 2.034$ feature of the peroxyl radical intermediate was observed at 0.3 s and disappeared by ~2 s in this reaction profile. The feature due to the glycyl radical lasted through 0.55 s and disappeared by 1.1 s. From 1.1 to 1.5 s, the coexistence of the peroxyl radical and the sulfinyl radical was observed. The rates of the formation and decay of the peroxyl radical intermediate in the acetylated enzyme were similar to those of free enzyme (Figure 7, panel b).

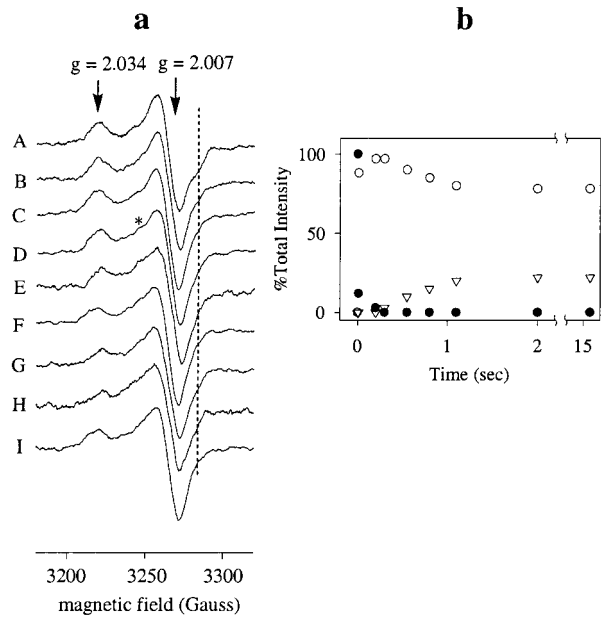

FIGURE 5: (a) Time-course of the oxygen inactivation of activated C419S PFL with oxygenated buffer. 56 μM active C419S PFL in anaerobic buffer (100 mM Hepes, 100 mM KCl, 6 mM DTT, pH = 7.5) was mixed at room temperature with 1 mM oxygenated buffer (100 mM Hepes, 100 mM KCl, pH = 7.5). The reaction was quenched at (A) 0.01 s, (B) 0.2 s, (C) 0.3 s, (D) 0.55 s, (E) 0.8 s, (F) 1.1 s, (G) 2.0 s, (H) 5.0 s, and (I) 15.2 s. The vertical dashed line indicates residual glycyl radical. The feature marked with (*) is tentatively assigned as a C418 based sulfinyl radical. (b) The time-course of % total intensity of each species (●, glycyl radical; ○, peroxyl radical; ▽, sulfinyl radical).

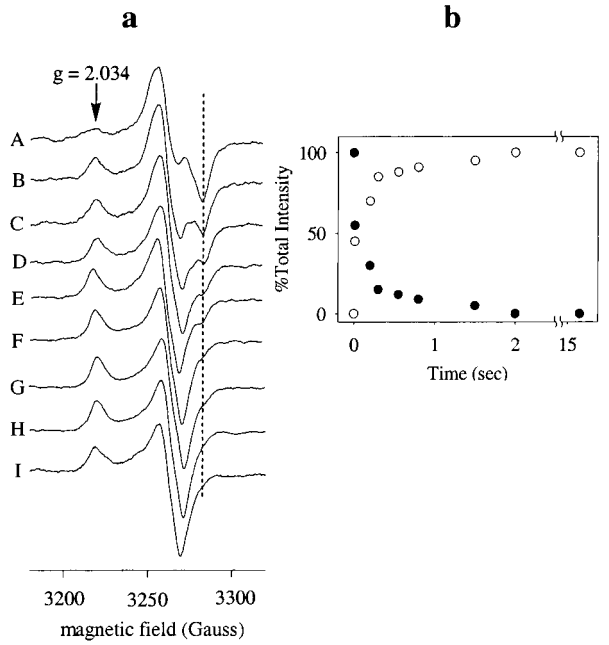

FIGURE 6: (a) Time-course of the oxygen inactivation of activated C418A/C419A double mutant PFL with oxygenated buffer. 56 μM active C418A/C419A double mutant PFL in anaerobic buffer (100 mM Hepes, 100 mM KCl, 6 mM DTT, pH = 7.5) was mixed at room temperature with 1 mM oxygenated buffer (100 mM Hepes, 100 mM KCl, pH = 7.5). The reaction was quenched at (A) 0.01 s, (B) 0.2 s, (C) 0.3 s, (D) 0.55 s, (E) 0.8 s, (F) 1.5 s, (G) 2.0 s, (H) 5.0 s, and (I) 15.2 s. The vertical dashed line indicates residual glycyl radical. (b) The time-course of % total intensity of each species (●, glycyl radical; ○, peroxyl radical).

DISCUSSION

In previous studies of the mechanism of oxygen inactivation of PFL (*15*), Reddy et al. observed a peroxyl radical (ROO•) in the C419A and the C418AC419A mutant PFLs, while only a sulfinyl radical was observed in wild-type PFL after ~30 s by manual freeze-quenching. The observation of a sulfinyl radical (RSO•) in C418A PFL indicated that C419 is the site of sulfinyl radical formation. These results indicated the potential involvement of at least two radical species during oxygen inactivation of PFL and suggested several mechanistic possibilities for the formation of sulfinyl radical. A mechanism (Scheme 1), in which the G734-based carbon centered peroxyl radical precedes formation of the C419-based sulfinyl radical, was favored on the basis of the predominant localization of the protein-based radical on the α-carbon of G734 and of the known rapid reaction of carbon radicals with dioxygen (*15*). In recent theoretical calculations, Gauld et al. also favored a scheme in which a carbon-centered peroxyl radical was formed first (*16*). The validity of this prediction was therefore tested in rapid freeze-quench studies presented here.

The results presented here unambiguously establish a peroxyl radical on the pathway to sulfinyl radical formation in wild type PFL. During oxygen inactivation of wild type PFL, a feature at $g = 2.034$, which is characteristic of the axial EPR spectra of peroxyl radicals, was clearly observed from the earliest time point after mixing (0.01 s) until 2 s and precedes formation of the sulfinyl radical (Figure 2). The half-life of the species giving rise to this feature is estimated to be ~1 s. At 2 s, the coexistence of these two radical species is evident, and the decay of the $g = 2.034$ feature is accompanied by an increase in the sulfinyl radical signal. These observations substantiated the earlier prediction

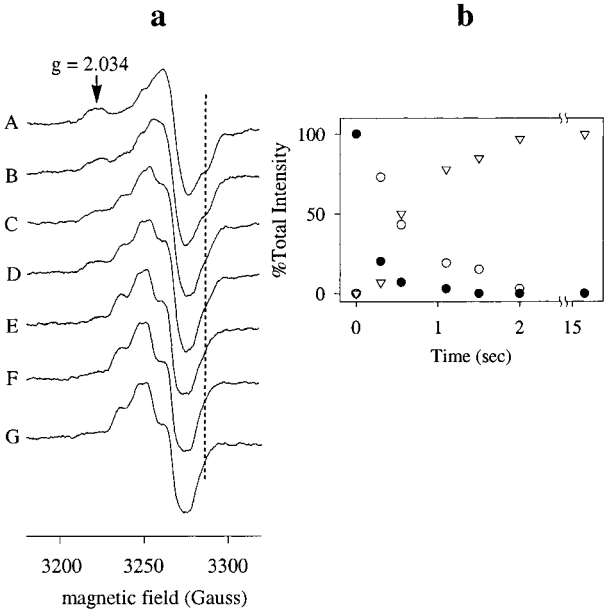

FIGURE 7: (a) Time-course of the oxygen inactivation of activated acetylated wild-type PFL with oxygenated buffer. 56 μM active acetylated wild-type PFL in anaerobic buffer (100 mM Hepes, 100 mM KCl, 6 mM DTT, pH = 7.5) was mixed at room temperature with 1 mM oxygenated buffer (100 mM Hepes, 100 mM KCl, pH = 7.5). The reaction was quenched at (A) 0.3 s, (B) 0.55 s, (C) 1.1 s, (D) 1.5 s, (E) 2.0 s, (F) 5.0 s, and (G) 15.2 s. The vertical dashed line indicates residual glycyl radical. (b) The time-course of % total intensity of each species (●, glycyl radical; ○, peroxyl radical; ▽, sulfinyl radical).

that, in wild-type PFL, a peroxyl radical is formed first, followed by formation of sulfinyl radical.

A peroxyl radical was also detected as an intermediate in the formation of sulfinyl radical during oxygen inactivation of C418A PFL (Figure 3). The kinetics of the reaction was essentially identical to wild-type PFL. Three important conclusions can be derived from this experiment: first, C419 is the site of sulfinyl radical formation confirming our earlier study (*15*); second, in the absence of C418, a peroxyl radical is formed that is kinetically identical with the formation of the peroxyl radical in wild type PFL; and third, C418 is not required for the kinetically competent conversion of the peroxyl radical to the sulfinyl radical.

Since there is little, if any, ambiguity about the nature of the carbon centered peroxyl radical in the C418AC419A, C419A, and C419S mutants of PFL, we reasoned that comparison of the kinetics of the formation of peroxyl radical in these proteins to those of wild type and C418A PFL would provide some evidence to support the assignment of the peroxyl radical observed in wild type and C418A enzymes (Figures 4−6). In the C419A, C419S, and C418A/C419A PFLs, the kinetics of peroxyl radical formation was nearly identical to wild type and C418A PFLs. This argues persuasively that the peroxyl radical observed in wild type and C418A PFLs are also carbon-centered radicals, consistent with earlier work (*15*, *16*).

Other lines of evidence support the formation of a peroxyl radical on G734 and not on C419 during the inactivation of wild type PFL. The thermodynamics of a glycyl/thiyl radical interchange in active PFL clearly favors the glycyl radical. Recent theoretical studies have estimated that the glycyl radical is favored thermodynamically by 3.4 kcal/mol, and the energy barrier for the direct transfer of hydrogen from C419 to the G734 radical is estimated to be ~9.9 kcal/mol (*22*). EPR data supports this qualitatively, since the glycyl radical is the only radical species that is observable in the resting active enzyme. Comparison of the EPR spectrum of the glycyl radical in wild-type PFL to the spectra for the mutant C419A, and the double mutant C419/A418A, by normalization and subtraction, reveals only residual intensity due to very small differences in line shape for the glycyl radicals in these PFLs and does not reveal a feature that would be indicative of any other radical being found in the wild-type spectrum and not in the mutants lacking C419 (data not shown). This approach was based on the hypothesis that some residual feature of the EPR signal of a putative thiyl radical might contribute to the intensity of active enzyme signal near $g = 2.0$ (*25*). In addition, EPR spectra recorded to lower field at 77 K did not reveal any additional features that could be assigned to another paramagnetic species. Finally, the work of Wagner et al. (*6*) demonstrated that the EPR spectrum of active wild type PFL could be effectively simulated using parameters consistent with a single glycyl radical species.

Since the second-order rate constants for the reaction of carbon radicals and of sulfur radicals with oxygen are similar, the relative rate of glycyl radical and thiyl radical reacting with dioxygen would be governed largely by the relative concentrations of these two species (*15*). Thus, the predicted >100-fold greater concentration of glycyl radical over thiyl radical under these conditions would appear to be the determining factor. An argument could be raised that, in the C419A and C418AC419A mutants, the truncation of C419 permits access of oxygen to G734 that is not available in wild type or C418A PFLs. However, the observation that the isosteric mutation C419S affords similar kinetics of peroxyl radical formation convincingly excludes the possibility of steric access as a determinant. This entire argument aside, it remains difficult to distinguish between a carbon-centered and sulfur-centered peroxyl radical by conventional continuous wave EPR spectroscopy as the *g* values of these two radicals are similar (*23*−*28*). Currently, several alternative RFQ-EPR approaches are underway in our laboratory to more clearly define the nature of the peroxyl radical in wild type and C418A PFL.

Reaction of PFL with pyruvate results in the formation of acetyl enzyme as an isolable intermediate. Knappe and coworkers had provided convincing evidence that C419 is the site of thiohemiketal formation with pyruvate and that C418 and C419 are sites of acetylation (*7*, *29*). Acetyl transfer to CoA, however, occurs from C418 (ref *7*, Kozarich, Wong, and Lewisch, unpublished results). This prompted us to propose a mechanism for catalysis that included a rapid acetyl exchange between C419 to C418 to account for the Knappe data. Recent work from the Knappe group has called their earlier work into question and suggests that C418 may be the sole site of thiohemiketal and acetyl group formation with C419 serving only as a radical-bearing intermediary in catalysis (*10*, *30*). Since acetylation at C419 might affect the kinetics of oxygen inactivation, we tested this possibility. The kinetics of the formation and decay of peroxyl radical and the formation of the sulfinyl radical in acetylated wild type PFL was similar to that of wild type PFL and not affected significantly by the acetylation of the enzyme (Figure 7). This result suggests that C418 may be the sole site of acetylation, which is consistent with our early findings in proton exchange studies (*8*). This result, however, cannot eliminate other mechanisms as it fails to rigorously rule out a fast transesterification equilibrium between C419 and C418. Clearly, more work is required on this point.

The proximity of G734 to C419 has biochemical and X-ray crystallographic support. Parast et al. demonstrated that C419 alone was responsible for the exchange of the α-carbon proton of glycyl radical with solvent (*8*). In addition, sulfinyl radical formation on C419 supports this as well (*15*). In a recent X-ray crystal structure of unactivated PFL, the Cα of G734 was found to be 3.72 Å away from the Sγ of C419 (Figure 8), with these two residues being located at the tips of two opposing hairpin loops (*10*). The Sγ of C418 was 7.42 Å away. Thus, direct chemistry between G734 and C419 is reasonable. It is interesting to note that both C419A and C419S PFLs reveal a slow conversion of the initially formed peroxyl radical to another radical as evidenced by the formation of a small shoulder to the low field side of the central feature (Figures 4 and 5) not seen in C418AC419A PFL (Figure 6). The shoulder is consistent with a slow formation of a sulfinyl radical at C418 that is constrained by the greater distance between this residue and G734. Therefore, the possibility of a direct radical transfer between G734 and C418 as an important step in the normal catalytic mechanism is remote.

Although we have no information on the stereochemistry of the peroxyl radical at G734, the possibility that both *R*- and *S*-isomers are formed cannot be excluded. If such were

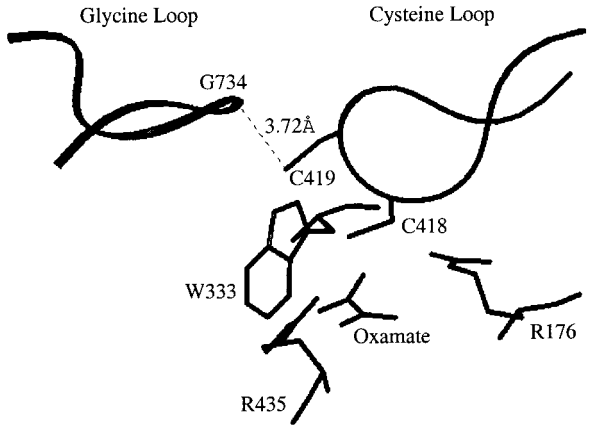

FIGURE 8: The active site of inactive wild-type PFL (adapted from Becker et al., ref *10*). The structure is drawn using InsightII software.

the case, however, the observed complete conversion of the peroxyl radical to the C419 sulfinyl radical would dictate that both isomers be accessible to reaction with this cysteine. Modeling the peroxyl moiety into the crystal structure revealed that the terminal oxygen of the S-isomer achieved a closest approach to the Sγ of C419 of 2.83 Å and the *R*-isomer, 4.85 Å without considering protein backbone flexibility (data not shown). Thus, if both isomers are formed, stereo randomness in the reaction with C419 is a reasonable explanation. This is consistent with our proposal explaining the C419-dependent solvent exchange at the α-hydrogen of G734 that required stereo randomness in the re-abstraction of hydrogen from G734 (*8*). For C418, the *S*- and *R*-isomers are 6.13 and 8.17 Å away, respectively. This would explain the greater stability of the peroxyl radical in C419A and C419S PFLs. In addition, the shoulder appearing on the low field side of the central feature in the EPR spectrum of these mutants appears to grow within 2 s and then stops increasing, suggesting the possibility of a stereochemical preference for the *S*-peroxyl radical by this cysteine. Resolution of this point awaits further experimentation.

Glycyl radical enzymes are an emerging class of anaerobic enzymes that perform a broad range of reactions (*2*, *31*). In 1988, we first suggested that the organic radical associated with PFL (at that time not known to be a glycyl radical) initiated catalysis by thiyl radical formation. Since then, the glycyl/thiyl radical equilibrium has been speculated about in two other glycyl radical-containing enzymes, anaerobic ribonucleotide reductase (*1*) and benzoyl succinate synthase (*2*). The glycyl/thiyl radical equilibrium is almost certainly a general feature in other proteins of this class of as yet unknown physiological function (*2*, *32*). The experiments reported here shed light on the specific chemistry of this new radical cofactor. Although the reaction investigated here is a side reaction leading to inactivation, it has proven to be valuable in understanding the spatial and mechanistic relationship of the active site glycyl radical to other active site residues. The discrimination in reactivity between C418 and 419 toward the G734 glycyl radical confirms under solution conditions with active PFL the spatial relationship of these residues observed crystallographically with inactive PFL. Recent X-ray crystallography studies with the anaerobic ribonucleotide reductase also suggests a similar spatial relationship between the active site glycine and a single active site cysteine residue (*33*). Therefore, the approach of RFQ-EPR with oxygen inactivation and the demonstration of the kinetic competence of the peroxyl radical reported here may provide a direct approach to confirm the reactive proximity and the identity of the glycine/cysteine pairs in other members of this class. We are currently turning RFQ-EPR methodology directly on the mechanism of catalysis by PFL using natural substrates as well as mechanism-based inactivators, such as acetylphosphinate (*8*, *34*), mercaptopyruvate (*35*), and fluoropyruvate (*36*). This should lead to a better understanding of the mechanism of this unusual family of enzymes.

ACKNOWLEDGMENT

We thank Drs. Boi Hanh Huynh, Dale E. Edmondson, and Carsten Krebs for their advice in the early setup of the anaerobic RFQ apparatus; Dr. Giovanna Scapin for her help on computer modeling studies; and Dr. M. D. Sevilla for a helpful discussion.

REFERENCES

1. Mulliez, E., Fontecave, M., Gaillard, J., and Reichard, P. (1993) *J. Biol. Chem. 268*, 2296−2299.
2. Leuther, B., Leutwein, C., Schulz, H., Horth, P., Haehenl, W., Schitz, E., Schagger, H., and Heider, J. (1998) *Mol. Biol. 28*, 615−628.
3. Knappe, J., Blaschkowski, H. P., Grobner, P., and Schmitt, T. (1974) *Eur. J. Biochem. 50*, 253−263.
4. Knappe, J., Neugebauer, F. A., Blaschkowski, H. P., and Ganzler, M. (1984) *Proc. Natl. Acad. Sci. U.S.A. 81*, 1332−1335.
5. Unkrig, V., Neugebauer, F. A., and Knappe, J. (1989) *Eur. J. Biochem. 184*, 723−728.
6. Wagner, A. F. V., Frey, M., Neugebauer, F. A., Schafer, W., and Knappe, J. (1992) *Proc. Natl. Acad. Sci. U.S.A. 89*, 996−1000.
7. Knappe, J., Albert, S., Frey, M., and Wagner, A. F. V. (1993) *Biochem. Soc. Trans. 21*, 731−734.
8. Parast, C. V., Wong, K. K., Kozarich, J. W., Peisach, J., and Magliozzo, R. S. (1995) *Biochemistry 34*, 2393−2399.
9. Leppanen, V.−M., Merckel, M. C., Ollis, D. L., Wong, K. K., Kozarich, J.W., and Goldman, A. (1999) *Structure 7*, 733−744.
10. Becker, A., Fritz−Wolf, K., Kabsch, W., Knappe, J., Schultz, S., and Wagner, A. F. V. (1999) *Nat. Struc. Biol. 6*, 969−975.
11. Sawers, G., and Bock, A. (1988) *J. Bacteriol. 170*, 5330−5336.
12. Sawers, G., and Bock, A. (1989) *J. Bacteriol. 171*, 2485−2498.
13. Conradt, H., Holman−Berger, M., Holmann, H. P., Blaschkowski, H. P., and Knappe, J. (1988) *Arch. Biochem. Biophys. 228*, 133−142.
14. Wong, K. K., Murray, B. W., Lewisch, S. A., Baxter, M. K., Ridkey, T. W., Ulissi DeMario, L., and Kozarich, J. W. (1993) *Biochemistry 32*, 14102−14110.
15. Reddy, S. G., Wong, K. K., Parast, C. V., Peisach, J., Magliozzo, R. S., and Kozarich, J. W. (1998) *Biochemistry 37*, 558−563.
16. Gauld, J. W., and Eriksson, L. A. (2000) *J. Am. Chem. Soc. 122*, 2035−2040.
17. Leppanen, V. M., Parast, C. V., Wong, K. K., Kozarich, J. W., and Goldman, A. (1999) *Acta Crystallogr. D. Biol. Crystallogr. 55*, 531−533.
18. Bradford, M. (1976) *Anal. Biochem. 72*, 248−254.
19. Hurshman, A. R., Krebs, C., Edmondson, D. E., Huynh, B. H., and Marletta, M. A. (1999) *Biochemistry 38*, 15689−15696.
20. Battino, R. (1981) *IUPAC Solubility Data Series*, Permagon Press, Oxford, U.K.

21. Chouchane, S., Lippai, I., and Magliozzo, R. S. (2000) *Biochemistry 39,* 9975−9983.
22. Himo, F., and Eriksson, L. A. (1998) *J. Am. Chem. Soc. 120,* 11449−11455.
23. Swarts, S., Becker, D., Debolt, S., and Sevilla, M. D. (1989) *J. Phys. Chem. 93,* 155−161.
24. Razskazovskii, Y., Colson A.-O., and Sevilla, M. D. (1995) *J. Phys. Chem. 99,* 7993−8001.
25. Sevilla, M. D., Yan, M., and Becker, D. (1988) *Biochem. Biophys. Res. Comm. 155,* 405−410.
26. Sevilla, M. D., Becker, D., and Yan M. (1990) *Int. J. Radiat. Biol. 57,* 65−81.
27. Becker, D., Summerfield, S., Gillich, S., and Sevilla, M. D. (1994) *Int. J. Radiat. Biol. 65,* 537−548.
28. Lacombe, S., Loudet, M., Cardy, H., and Dargelos, A. (1999) *Chem. Phys. 244,* 175−183.
29. Plaqa, W., Frank, R., and Kanppe, J. (1988) *Eur. J. Biochem. 178,* 445−450.
30. Plaga, W., Vielhaber, G., Wallach, J., and Knappe, J. (2000) *FEBS Lett. 466 (1),* 45− 48.
31. Eklund, H., and Fontecave, M. (1999) *Structure Fold Des. 7 (11),* R257−262.
32. Sawers, G., and Watson, G. (1998) *Mol. Microbiol. 29 (4),* 945−954.
33. Logan, D. T., Anderson, J., Sjoberg, B.-M., and Nordlund, P. (1999) *Science 282,* 1499−1504.
34. Ulissi-DeMario, L., Brush, E. J., and Kozarich, J. W. (1991) *J. Am. Chem. Soc. 113,* 4341−4342.
35. Parast, C. V., Wong, K. K., Kozarich, J. W., Peisach, J., and Magliozzo, R. S. (1995) *Biochemistry 34,* 5712−5717.
36. Parast, C. V., Wong, K. K., Kozarich, J. W., Peisach, J., and Magliozzo, R. S. (1995) *J. Am. Chem. Soc. 117,* 10601−10602.

BI002589K